Analysis of self-heating and trapping in organic semiconductor devices

Evelyne Knapp ; Beat Ruhstaller;

Analysis of self-heating and trapping in organic semiconductor devices. Proc. SPIE 9566, Organic Light Emitting Materials and Devices XIX, 95660X (September 22, 2015);

Evelyne Knapp, Zurich Univ. of Applied Sciences (Switzerland)
Beat Ruhstaller, Zurich Univ. of Applied Sciences (Switzerland)
Fluxim AG (Switzerland)

Published in SPIE Proceedings Vol. 9566:

Organic Light Emitting Materials and Devices XIX

Analysis of self-heating and trapping in organic semiconductor devices

Evelyne Knapp[a] and Beat Ruhstaller[a,b]

[a]Zurich University of Applied Sciences, Institute of Computational Physics, Wildbachstr. 21, 8400 Winterthur, Switzerland;
[b]Fluxim AG, Technoparkstr. 2, 8406 Winterthur, Switzerland

ABSTRACT

So far self-heating has only been of concern in large-area devices where the resistive transparent anode leads to a potential drop over the device resulting in inhomogeneous current, brightness and temperature distributions. In this work, we show that even small lab devices suffer from self-heating effects originating from the organic semiconductor layer. In admittance spectroscopy of organic semiconductor devices, negative capacitance values often arise at low frequency and high voltages. In this study we demonstrate the influence of self-heating on organic semiconductor devices with the aid of a numerical 1D drift-diffusion model that is extended by Joule heating and heat conduction. Furthermore the impact of trap states on the capacitance in combination with self-heating is demonstrated. The typical signature of self-heating might be overshadowed depending on the trapping dynamics. In a next step, we compare the negative capacitance vs. frequency for uni- and bipolar devices to quantify the different processes. We emphasize the impact of self-heating and trapping on OLEDs and organic solar cells. To ease the interpretation of the results we investigate simulations in the time domain as well as in the frequency domain. We have provided clear evidence of self-heating of organic semiconductor devices and conclude that a comprehensive model requires the inclusion of heat conduction and heat generation in the drift-diffusion model.

Keywords: negative capacitance, self-heating, OLED, simulation, trap states

1. INTRODUCTION

As opposed to inorganic LEDs where the thermal management is an important issue for organic light-emitting devices (OLEDs) no heat sink is needed. Nevertheless heat is also generated in OLEDs. Heat disspation affects display applications,[1] but especially lighting applications.[2] The impact of self-heating of OLEDs has mainly been investigated in large-area devices.[3,4] In such devices the transparent anode is resistive leading to Joule heating, and thus to a potential drop over the electrode. The potential drop results in an inhomogeneous brightness distribution over the device. Only recently the impact of self-heating of the organic semiconductor material has been studied as in reference[5] where current-voltage curves are simulated and compared with measurements. The model includes self-heating in the organic semiconductor layer with a temperature-dependent mobility. We show that the influence of self-heating on small OLEDs becomes even more distinct when time-dependent measurements are employed. Typical measurements of capacitance vs. frequency and capacitance vs. voltage plots are shown in Fig. 1. The negative capacitance effect becomes stronger with applied bias. In the C-V plot the negative capacitance increases with lower frequency. Similar experiments are conducted in references[6,7] where with the aid of admittance spectroscopy negative capacitance values were found in uni- and bipolar devices. Such findings were previously assigned to interfacial effects,[8,9] recombination[10,11] or trap states. The authors of reference[6] show that the negative capacitance effect can be decreased by adding a copper block on top of the device leading to a lower internal device temperature. It was demonstrated in reference[7] that this behaviour can be reproduced with the aid of simulation by including the heat equation to the drift-diffusion model. No other model ingredients such as trap states or interfacial states were introduced.

Further author information: (Send correspondence to Evelyne Knapp.)
Evelyne Knapp: E-mail: evelyne.knapp@zhaw.ch, Telephone: +41 (0)589346757
Beat Ruhstaller: E-mail: beat.ruhstaller@zhaw.ch, Telephone: +41 (0)589347836
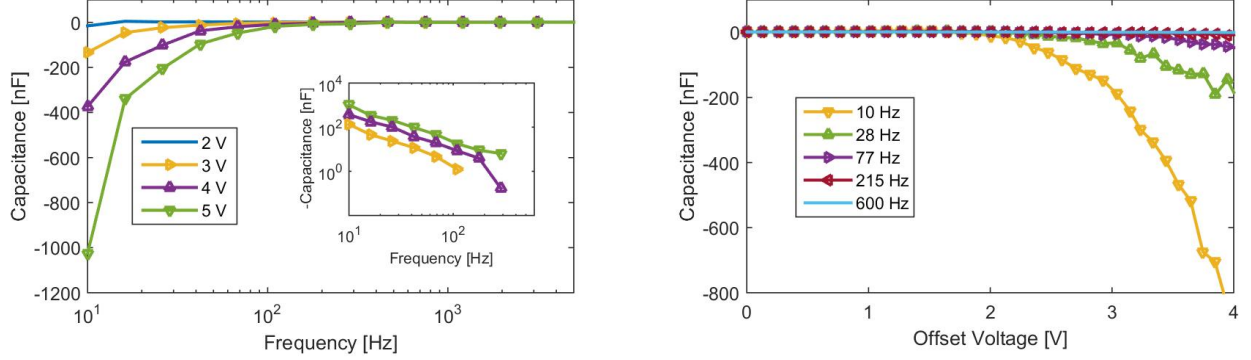
Figure 1: A C-f on the left and C-V measurement on the right of a single layer hole-only device. The negative capacitance effect enhances with increasing bias. The inset on the left shows the negative capacitance in log-log representation. On the right the negative capacitance effect becomes more pronounced with low frequency.

2. MATHEMATICAL MODEL

We investigate a hole-only device with a one dimensional drift-diffusion model.[7] The organic semicondutor layer is sandwiched between the anode and cathode. The model consists of the Poisson equation (1) for the hole density p and the trap states p_t as well as the potential ψ:

$$\nabla \cdot (\epsilon_0 \epsilon_r \nabla \psi) = q(-p - p_t) \tag{1}$$

$$J_p = -qp\mu\nabla\psi - qD\nabla p \tag{2}$$

$$\nabla \cdot J_p + q\frac{\partial p}{\partial t} = 0. \tag{3}$$

The vacuum permittivity is denoted by ϵ_0, the relative permittivity by ϵ_r and the elementary charge by q. The continuity equation is given by Eq. (3) with the current density J_p as described by Eq. (2). The mobility of the organic semiconductor is denoted by μ.

For simplicity, we assume fixed charge carrier densities at the anode (4) and cathode (5). For a device with thickness L and with N_0 the number of sites we can write

$$p(0) = N_0, \tag{4}$$

$$p(L) = N_0 \exp\left(-\frac{qV_{bi}}{kT}\right) \tag{5}$$

where the built-in voltage is denoted by V_{bi}.

The trap states and free charge carriers interact according to the kinetic equation:

$$\frac{\partial p_t}{\partial t} = c_p p[N_t - p_t] - e_p p_t. \tag{6}$$

The capture coefficent is denoted by c_p and is linked to the escape rate e_p assuming a single trap level E_t in the following way:

$$e_p = c_p N_0 \exp\left(\frac{E_{HOMO} - E_t}{kT}\right). \tag{7}$$

The classical drift-diffusion model (1-3) is restricted to the organic semiconductor layer of the hole-only device.

To include thermal effects the electrical model is extended by the heat equation (8) where the temperature is denoted by T. The thermal model comprises the entire domain of the hole-only device, i.e. including glass, electrodes and air gap. We assume that heat transfer in the device takes place by thermal conduction and that thermal exchange with the surrounding is based on convection and thermal radiation. The Joule heat source term[12] $J_p^2/(q\mu p)$ lies in the organic semiconductor layer and is proportional to the electrical resistance of the material. In the other layers there is no heat source, only heat conduction. The continuity equation for heat conduction is given in the following:

$$c\rho \frac{\partial T}{\partial t} = \quad \nabla \cdot (k\nabla T) + \frac{J_p^2}{q\mu p} \tag{8}$$

the parameter c stands for the specific heat capacity, ρ for the density and k for the thermal conductivity.

Convective and radiative boundary conditions are used in the thermal model. The heat flux density F is calculated from the heat transfer coefficient h and the ambient temperature T_{ref}, further the emissivity is given by ϵ and the Stefan-Boltzmann constant by σ:

$$F = -k\nabla T = -h(T - T_{ref}) - \epsilon\sigma(T^4 - T_{ref}^4). \tag{9}$$

We assume the same temperature for the convective air flow as for the ambient.

Note that we assume a temperature independent mobility μ whereas the diffusion D increases with an enhanced temperature since D is proportional to the temperature T

$$D = \frac{kT}{q}\mu. \tag{10}$$

Using a temperature-dependent mobility $\mu(T)$ would intensify the negative capacitance effect, but is not considered here for simplicity. If a strong temperature dependence of the mobility is present thermal run-away may result in catastrophic failure of the device.

3. METHODS AND RESULTS

A numerical sinusoidal small signal analysis (S^3A) was performed as in reference[13] to calculate the frequency-dependent impedance $Z(\omega)$ and admittance $Y(\omega)$ which is defined as $Z = \frac{V^{ac}}{I^{ac}}$ and $Y = \frac{I^{ac}}{V^{ac}}$, respectively. The determination of the ac current response I^{ac} to a harmonic voltage modulation $V^{ac} = V_{offset} + V_0\cos(\omega t)$ has therefore to be calculated. The frequency-dependent admittance $Y(\omega)$ can then by decomposed into the conductance G and capacitance C according to $Y(\omega) = G(\omega) + i\omega C(\omega)$ while the impedance $Z(\omega)$ consists of the resistance R and the reactance X as stated below

$$Z(\omega) = R(\omega) + iX(\omega). \tag{11}$$

In this work, we will focus on the capacitance C and investigate situations where the capacitance is decreased at low frequency due to self-heating in the device as shown in Fig. 1. On the other hand an increased capacitance at low frequency can be found due to trap states.[14]
In Fig. 2 on the left the capacitance for two different HODs are shown. The only difference in the two simulations is the capture coeffcient c_p. This coefficent influences the trapping dynamics in Eq. (6). Varying the capture coefficient c_p changes the values of the capacitance at low frequency dramatically. For fast trapping we get an negative capacitance as for trapfree devices as explained in reference[7] in more details. For small capture coeffcents however the capacitance is enhanced at low frequencies. The question arises why the influence of self-heating on the capacitance is not visible with its typical signature. We therefore simulate the dark injection transient currents (DITC) for the two devices in Fig. 2 on the right. A voltage step from 6 to 6.1 V is applied. In the case of fast trapping (red line) the charge carriers are quickly released after the DIT peak and the current density rises again at around 100 s to its final steady-state value. This is due to self-heating. In the case of slow trapping (dashed line) the self-heating induced current rise is overshadowed by the trapping process. Although
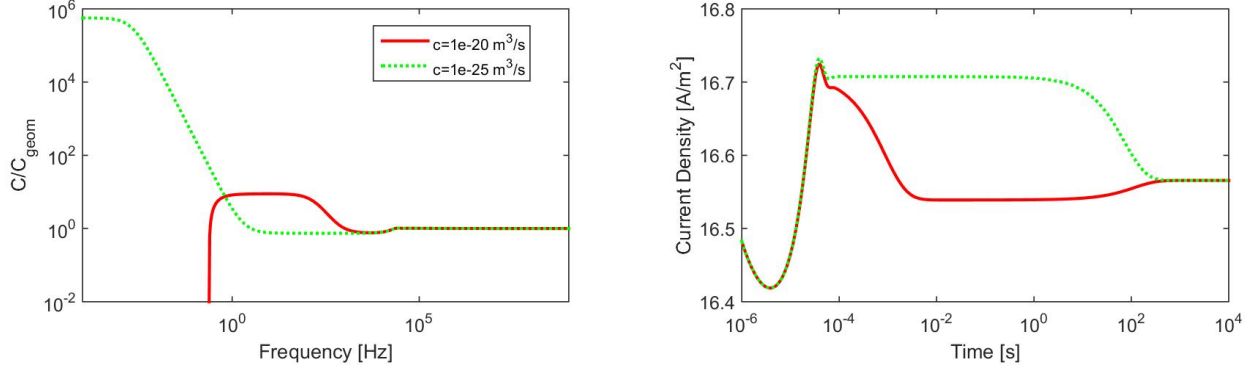
Figure 2: Depending on the capture rate c_p the characteristics of the self-heating shows up in a totally different way. On the left: simulated capacitance vs. frequency plots for two devices with different capture coefficents c_p at 6 V. Varying the capture coefficent leads to a negative or enhanced capacitance value at low frequencies. Simulated dark injection transient currents for the same devices with different capture coefficents c_p and an applied voltage step from 6 V to 6.1 V are shown on the right. The self-heating induced current density rise is overshadowed by trapping.
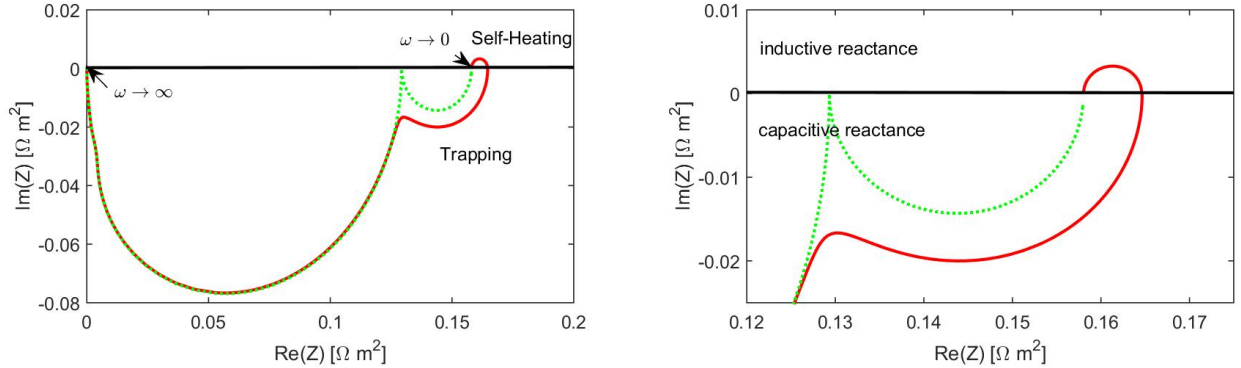

Figure 3: Impedance representation of the same devices. On the left the impedance for high frequencies is plotted near the origin. A zoom-in of the low frequency regime is displayed on the right side. Note the difference between the two curves at low frequencies. The negative capacitance regime is represented in the positive plane of the impedance plot.

self-heating is not visible with its characteristic signature it is nevertheless present. Interestingly, the steady-state current voltage curves of the two device are identical as the steady-state value in Fig. 2 on the right is the same. Only the dynamic characterisation reveals the difference in charge trapping kinetics. Fig. 3 shows the original representation of the impedance $Z(\omega)$ where the real and imaginary parts are plotted. The red line shows again the result for fast trapping and the dashed line for slow trapping. The high frequency regime is located near the origin while the low frequency regime is on the right side. For the ease of interpretation a zoom-in is displayed in Fig. 3. The impedance $Z(\omega)$ for low frequencies is shown on the right side in the picture where the red and dashed line differ the most. The change in sign is also visible. At low frequency the green line is below 0, while the red line is above it. On the left side, close to the origin, or at high frequencies the two curves are identical. If the admittance is expressed in terms of resistance R and reactance X we obtain $Y(\omega) = G + i\omega C = Z^{-1} = (\frac{1}{R^2 + X^2})(R - iX)$. From this we see that the capacitance will have the opposite sign of the reactance.

In Fig. 4 a diagramm for the interpretation of Fig. 3 is displayed. The sign of the reactance determines the behaviour of the OLED. In the case of a positive sign of the reactance, a positive phase angle and phase shift is obtained. In the case of a negative sign, a negative phase shift is given. On the right side the phase shifts are
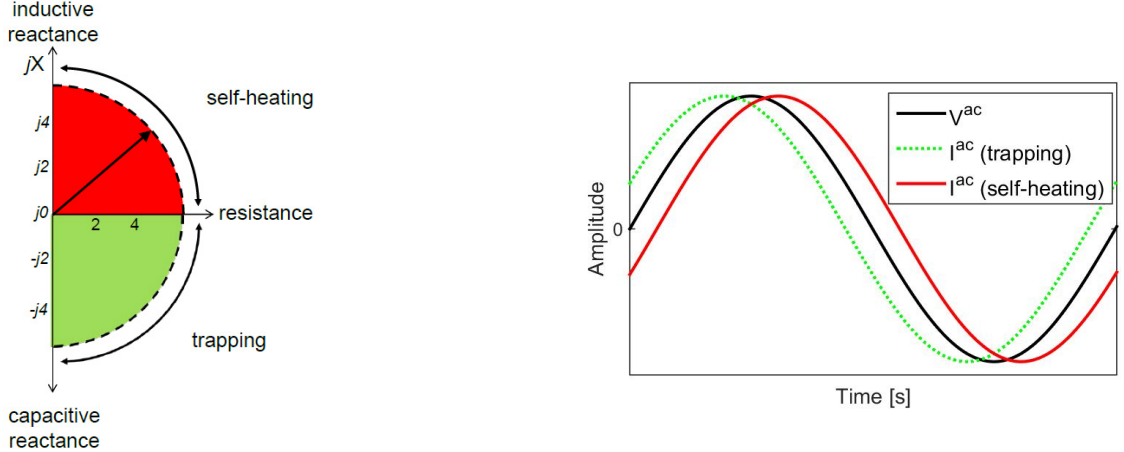
Figure 4: Interpretation of impedance in the presence of self-heating and trapping. On the left the complex impedance is split in capacitive and inductive reactance. On the right the phase shift is visualized (not to scale).

plotted (not to scale). In the case of self-heating the current lags behind the voltage because of heat-induced current rise, while in the case of trapping the current leads the voltage because of trapping-induced reduction of current. The transient behaviour of the device is thus changed.

We now investigate a bipolar sample device. For the bipolar simulations we extend the model in section 2 for electron transport and introduce a Langevin recombination term of the following form:

$$R\frac{q}{\epsilon_0\epsilon_r}(\mu_p + \mu_n)np \tag{12}$$

The prefactor R stands for the recombination strength and is varied from 0.01 to 1. In the heat equation (8) an additional Joule heating terms for electrons is considered. Note that only Joule heating and no other heat generation as e.g. recombination heat is simulated. In Fig. 5 two simulation types are displayed. We plot the absolute value of the calculated normalized capacitance. First, the device is kept at 300 K and no self-heating takes place. The dashed lines show that with a decreasing prefactor R the negative capacitance effect becomes stronger. The impact of the recombination strength on the capacitance is clearly visible as explained in more detail in reference[11] where the recombination strength is estimated with the aid of impedance spectroscopy. Secondly, a device with self-heating is simulated. The negative capacitance effects becomes even more pronounced with self-heating. The self-heating induced change in the negative capacitance however sets in at lower frequency than the recombination effect. As a reference the unipolar results are also shown where no recombination takes place. Notice that only the organic material is simulated and no additonal layers.

4. CONCLUSIONS

We have introduced a model description that shows that self-heating plays a major role, even in small-area organic devices. Different characterization techniques are presented to identify self-heating. Steady-state current-voltage curves do not show clear indications of self-heating. Dynamic characterization methods are more suitable. Identifying the self-heating induced current rise in DITC experiments can be difficult depending on the applied voltage and cooling of the device. The signature of self-heating is most easily dedectable in IS measurements in terms of the negative capacitance at low frequency and high bias. However note that self-heating and trapping are competing processes and may overshadow one another. Trapping will phase shift the current density response in the opposite direction than self-heating with respect to the input voltage signal. Simulating bipolar devices reveals two sources for the negative capacitance. In addition to self-heating also the recombination prefactor influences the space charge and leads to a negative capacitance. The negative capacitance effects however set in at different frequencies. In conclusion, the simulations show the importance of self-heating in small devices and confirm self-heating as origin of negative capacitance, especially in unipolar devices. Depending on the structure
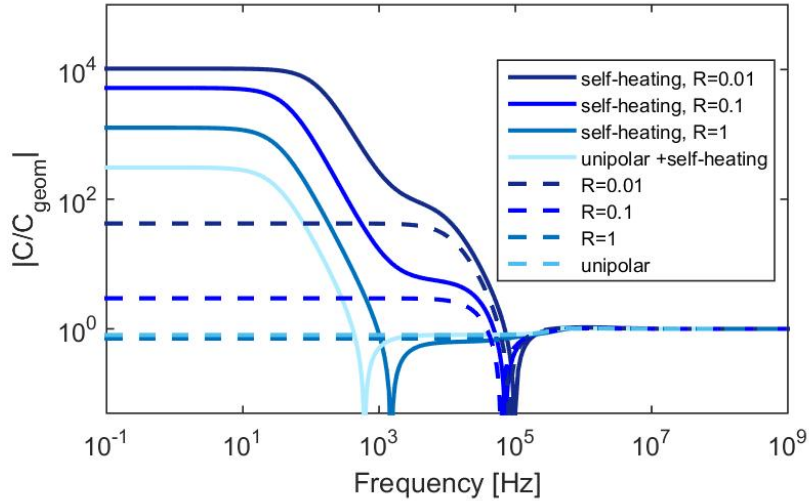
Figure 5: Simulation of bipolar device with and without self-heating effects.

of the samples, this might lead to undesired effects in the performance. Heat dissipation should be taken into account when fabricating organic semiconductor devices and be considered in any electrical characterization technique regardless of dc, ac, or transient.

REFERENCES

[1] J. Sturm, W. Wilson, and M. Iodice, "Thermal effects and scaling in organic light-emitting flat-panel displays," *IEEE Journal of Selected Topics in Quantum Electronics* **4**, pp. 75–82, Jan 1998.

[2] K. Hayashi, H. Nakanotani, M. Inoue, K. Yoshida, O. Mikhnenko, T.-Q. Nguyen, and C. Adachi, "Suppression of roll-off characteristics of organic light-emitting diodes by narrowing current injection/transport area to 50nm," *Applied Physics Letters* **106**(9), p. 093301, 2015.

[3] M. Slawinski, D. Bertram, M. Heuken, H. Kalisch, and A. Vescan, "Electrothermal characterization of large-area organic light-emitting diodes employing finite-element simulation," *Org. Electron.* **12**, p. 13991405, 2011.

[4] S. Harkema, S. Mennema, M. Barink, H. Rooms, J. S. Wilson, T. van Mol, and D. Bollen, "Large area ito-free flexible white oleds with orgacon pedot:pss and printed metal shunting lines," in *Organic Light Emitting Materials and Devices XIII, Proc. SPIE* **7415**, 2009.

[5] A. Fischer, T. Koprucki, K. Grtner, M. L. Tietze, J. Brckner, B. Lssem, K. Leo, A. Glitzky, and R. Scholz, "Feel the heat: Nonlinear electrothermal feedback in organic leds," *Advanced Functional Materials* **24**(22), pp. 3367–3374, 2014.

[6] H. Okumoto and T. Tsutsui, "A source of negative capacitance in organic electronic devices observed by impedance spectroscopy: Self-heating effects," *Appl. Physics Express* **7**, p. 061601, 2014.

[7] E. Knapp and B. Ruhstaller, "Analysis of negative capacitance and self-heating in organic semiconductor devices," *J. Appl. Phys.* **117**, p. 135501, 2015.

[8] G. Garcia-Belmonte, J. Bisquert, P. R. Bueno, and C. Graeff, "Impedance of carrier injection at the met-alorganic interface mediated by surface states in electron-only tris(8-hydroxyquinoline) aluminium (alq3) thin layers," *Chemical Physics Letters* **455**(46), pp. 242 – 248, 2008.

[9] G. Garcia-Belmonte, J. Bisquert, P. R. Bueno, C. Graeff, and F. Castro, "Kinetics of interface state-limited hole injection in -naphthylphenylbiphenyl diamine (-npd) thin layers," *Synthetic Metals* **159**(56), pp. 480 – 486, 2009.

[10] N. D. Nguyen, M. Schmeits, and H. P. Loebl, "Determination of charge-carrier transport in organic devices by admittance spectroscopy: Application to hole mobility in -npd," *Phys. Rev. B* **75**, p. 075307, Feb 2007.

[11] H. H. P. Gommans, M. Kemerink, and R. A. J. Janssen, "Negative capacitances in low-mobility solids," *Phys. Rev. B* **72**, p. 235204, Dec 2005.

[12] J. Piprek, *Semiconductor Optoelectronic Devices: Introduction to Physics and Simulation*, Academic Press, 2013.

[13] E. Knapp and B. Ruhstaller, "Numerical impedance analysis for organic semiconductors with exponential distribution of localized states," *Appl. Phys. Lett.* **99**, p. 093304, 2011.

[14] E. Knapp and B. Ruhstaller, "The role of shallow traps in dynamic characterization of organic semiconductor devices," *J. Appl. Phys.* **112**, p. 024519, 2012.